IJCRT.ORG ISSN : 2320-2882

INTERNATIONAL JOURNAL OF CREATIVE RESEARCH THOUGHTS (IJCRT)
An International Open Access, Peer-reviewed, Refereed Journal

# CORRELATION BETWEEN FORCED AND PERFORMANCE-BASED SEISMIC DESIGN FOR IRREGULAR STRUCTURES

[1] Ahmed Mabrouk, [2]Ayman Embaby, [3]Ayman Khalil

[1]Post graduate student, [2]Professor of structural engineering, [3]Professor of structural engineering
[1] Department of Structural Engineering,
[1] Ain Shams University, Cairo, Egypt

***Abstract:*** Seismic design codes are generally based on strength philosophy, where structures are designed on a linear elastic force-based design (FBD) approach. The main objective of this philosophy is a strength rather than a displacement capacity. This paper reviews the Egyptian code-compliant designs (CCD) to test their effectiveness, reliability, and structural performance, as well as it proposes an alternative performance-based design (PBD) approach for seismic design, by developing a performance factor (P) for different performance levels. Regular and irregular RC moment frame structures are assessed using this approach through nonlinear static pushover analysis. The correlation between forced based and performance-based design methods is carried out using the performance factor (P), which can be used in design codes to have a more reliable fulfillment of intended seismic performance and reduced construction costs while accommodating to the owner's features.

***Index Terms* - Seismic analysis; Performance factor; Irregular structures; RC moment frames; Nonlinear analysis; Pushover Analysis**

## 1. INTRODUCTION

Researchers have been trying to improve the methodologies and techniques used in seismic assessment and design of structures in recent years to capture the structure's exact behavior under seismic effects. Structural performance concept has been introduced to evaluate the adequacy of the existing structures or even design new structures under seismic effects; this can be shown in the different and vast standards and guidelines that have been introduced throughout the years (ASCE, 2007, 2014; ATC, 1996; FEMA, 1997, 2000, 2005; LATBSDC, 2018; TBI, 2017). All these standards and guidelines adopt the concept of nonlinear analysis of the structure to have a better realistic perception of the structure behavior and deliver answers for questions regarding the expected damage of the structures and the safety levels of code-compliant design (CCD) structures. Construction of high-rise buildings around the world have led researchers to focus on finding a more cost-effective design approaches which cannot be found in current force-based design codes, that's why extensive research efforts have focused on the behavior of the structures using nonlinear analysis procedures that can predict the performance level of the structure (immediate occupancy level, life safety level, Collapse prevention level).

Researchers in the past have studied the performance and responses of different structures. Work done by (Mehanny & El Howary, 2010) to study and evaluate the Egyptian seismic code provisions for low- to mid-rise (4- and 8-story) RC moment frames, through a series of static inelastic pushover and nonlinear incremental dynamic analyses shows that the code provisions results in moment frames that are life safe and satisfies various seismic performance levels (e.g. IO, LS, and CP) corresponding to relevant seismic hazard levels while recommending a special emphasis to reduce the R-value for the perimeter frame configuration as they are more vulnerable and more prone to exceed LS and CP performance levels than the space frames. (Jiang, Lu, & Zhu, 2012) have indicated how a performance-based design (PBD) approach can demonstrate the safety of code-exceeding tall buildings violating the code extent of irregularity or height. Also, the study done by (A. Mwafy, 2013) shows the effect of using inelastic analysis tools in design to have different structures with similar reliability and cost-effectiveness. Furthermore, (Chaulagain et al., 2014) have demonstrated the ductility and overstrength of representative irregular RC buildings in Kathmandu valley in Nepal, showing the negative effect of irregularity on the structure performance. This study assesses the performance of the Egyptian CCD and presents a new factor that can be used in the design of different RC structures, namely the performance factor (P) that depends on the intended seismic performance level.

Nonlinear time history analysis is a powerful tool to study the structural response, but it has several drawbacks regarding its computational effort and time-consuming that makes its practical use very difficult. That's why nonlinear static procedures (NSPs) have been used in the past years instead of time history analysis to overcome its drawbacks; several studies were developed demonstrating the good performance of NSPs on the seismic performance of structures (Augusto & Bhatt, 2011; Belejo & Bento, 2015; A. M. Mwafy & Elnashai, 2001). Also, several standards and guidelines recommend using NSPs methods as an assessment method, among other analysis procedures (ASCE, 2014; FEMA, 2005). The NSPs is selected for this study for its applicability to PBD philosophy (Krawinkler &

Seneviratna, 1998), and simplicity where the structure is subjected to a monotonic load (forces or displacements) representing seismic action, with an invariant or adaptive pattern, that is incrementally applied to the structure. This analysis also includes gravity loads. The outcome of the pushover analysis is the pushover curve (capacity curve), which represents the variation of the base shear (*V*) with the roof displacement (*D*) in a selected controlled node. In this study, a wide set of medium and high-rise RC moment frame structures of different properties are analyzed in the elastic and inelastic stages using three-dimensional (3D) models where their capacity and susceptibility to deterioration is examined as the structure is pushed laterally till collapse to estimate its performance and identify any weak or vulnerable structural members, after which the performance level of the structure is investigated. This simple process of pushing the structure and studying its behavior in the nonlinear stage will lead to a more refined analysis and design eventually.

## 2. CURRENT SEISMIC CODES PROCEDURES

The seismic design has been generally based on strength, where structural elements members are assessed based on stresses caused by equivalent seismic forces. The most popular procedure used in this philosophy is considered to be the response spectrum analysis which is used by most design codes, where the structure is considered to be linear elastic but the forces in the structure is divided by a response modification factor (R), to approximately account for the structure nonlinear behavior, as shown in Figure 1. The value of the ‘R’ factor in different codes mainly depends on the lateral resisting system, and the structural geometry, below in Table 1 are some of the ‘R’ factor values that can be found in different codes and standards (ASCE, 2017a; CEN, 2004; ECP, 2012; International Conference of Building Officials, 1997) for RC moment frames.

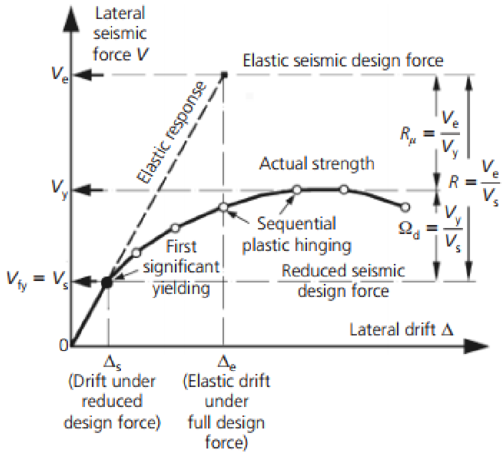


Figure 1 Inelastic force-deformation curve

Table 1 ‘R’ Factor in different codes and standards

| Structural system | R factor | | | |
|---|---|---|---|---|
| | ECP-201 | Eurocode 8 | UBC 97 | ASCE 7-16 |
| RC moment frames with Limited ductility | 5 | - | - | - |
| RC moment frames with sufficient ductility | 7 | - | - | - |
| RC moment frames with medium ductility | - | 3,0 $\alpha_u/\alpha_I$ | - | - |
| RC moment frames with high ductility | - | 4.5 $\alpha_u/\alpha_I$ | - | - |
| Concrete ordinary moment-resisting frames (OMRF) | - | - | 4.5 | 3.0 |
| Concrete intermediate moment-resisting frames (IMRF) | - | - | 5.5 | 5.0 |
| Concrete Special moment-resisting frames (SMRF) | - | - | 8.5 | 8.0 |

The value of the ‘R’ factor could differ from one code to the other, but the same methodology is common between them, which is based on FBD philosophy. A critical review of this philosophy drawbacks was published by (Priestley, 2003), as it is necessary to understand that a single average number cannot entirely represent the inelastic behavior for different structures (Fajfar, 2018). That’s why the need to change the methodologies used of seismic design is an essential process, and one of the main ideas is that design to be based on performance and analyzing damage and collapse patterns to reach a reliable and sustained structural behavior better. The codes, as mentioned earlier and standards, offer certain restrictions when designing irregular structures to account for their negative impacts on structural performance. However, it is essential to understand that the performance of irregular structures is unpredictable and ignoring their effect may lead to structural damage, for this reason, this study presents the effect of certain types of irregularities on the structural behavior separately.

## 3. METHODOLOGY

Although nonlinear methods can capture the actual structure behavior and can lead to a better and a more reliable design, but using these methods is not a popular option to different design firms and consultancy offices around the world maybe because that they demand more time and iterations than linear elastic design or possibly due to the lack of experience in this field. Traditionally designers are more familiar FBD concept, which mainly depends on the ‘R’ factor, knowing that this philosophy may yield in a vague and unpredictable performance. In this study, a review of structures’ performance designed according to the current code requirement is investigated. Also, a new attempt to develop the ‘R’ factor is introduced to account for different performance levels by using the ‘P’ factor. The same philosophy that is used in calculating the ‘R’ factor, which mainly depends on the structure ductility ‘μ’ and overstrength ‘Ω’ is used in this study for calculation of the performance factor ‘P’ that will be calculated for different RC moment frame structures ranging between regular and irregular ones. The different types of irregularities that shall be examined in this study are:

1- Vertical geometric irregularity due to the story’s setbacks
2- Stiffness irregularity (soft-story) due to the story’s variable heights

3- Weight (mass) irregularity due to mass concentration at different floors

All the above-mentioned types of irregularities are only some of the ones that were stated in various codes and standards, including Egyptian code (ECP, 2012). The types of irregularities investigated in this study were selected based on their popular existence in our structures, and to emphasize their effect on structure performance. Performance philosophy depends on two factors mainly; the first one is the seismic demand which can be defined by a series of earthquake accelerograms or a response spectrum and the second one is the structural capacity (pushover curve), which can be defined as the structure's ability to resist the demand. And to reach a certain performance level, the structural capacity must handle the demand and be capable of withstanding it. The basic performance levels that are being investigated in this study are compatible with the performance levels that are defined in different standards as the ones found in (ASCE, 2017b; ATC, 1996; béton, 2003) these levels are as follows:

- Operational Level (OP)
- Immediate Occupancy Level (IO)
- Life Safety Level (LS)
- Collapse Prevention Level (CP)

, what varies between these levels is the severity and overall damage of structural and nonstructural components.

Different state-of-the-art methodologies have been published to assess the structure performance adopting the NSPs concept. The target displacement method in ASCE standards (ASCE, 2014) is the one used in this study to determine the structures' performance levels along with the drift limits in ATC 40 (ATC, 1996) for different performance levels.

### 3.1. Calculation of the Performance factor

The procedure used in this study to calculate the 'P' factor is matching with the one used to calculate the 'R' factor, this method is intended to be used for structures with different performance and ductility levels, to be able to use this factor in the design of new structures. 'R' factor can be expressed as the ratio between the maximum lateral force that the structure can withstand under a linear elastic behavior '$V_e$,' to the lateral force '$V_d$.' Ductility 'μ' and overstrength 'Ω' are the two main factors affecting the value of the 'R' factor, the basic formula for establishing the 'R' factor can be shown in Equation 4 (Uang, 1991). The method used in this study in calculating the 'R' factor is similar to the recommended methodology found in FEMA P695 (ATC, 2009), as shown in Figure 2, which focuses on the ductility and overstrength factors and assumes 'R' to be the product of these two terms only as the redundancy factor is considered unity.

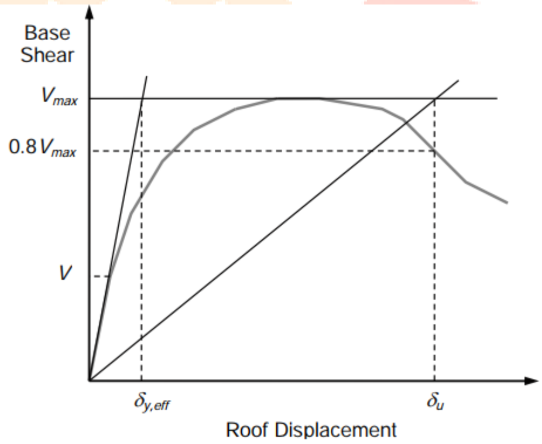


Figure 2 Idealized nonlinear static pushover curve

FEMA P695 consider the ductility factor 'μ' as the ratio between the ultimate roof drift displacement until a loss of 20% of the base shear capacity (0.8 $V_{max}$) is achieved, $\delta_u$ to the effective yield roof drift displacement $\delta_{y,eff}$ as shown in Equation 1:

$$\mu = (\delta_u / \delta_{y,eff}) \quad (1)$$

The effective yield roof drift displacement can be calculated through Equation 2:

$$\delta_{y,eff} = C_0 \ (V_{max} / W) \ (g/4\pi^2) \ (\max(T,T_1))^2 \quad (2)$$

where $C_0$ is based on Equation C3-4 of ASCE/SEI 41-06, $V_{max}/W$ is the maximum base shear normalized by building weight, g is the gravity constant, T is the fundamental period based on the empirical formulas, and $T_1$ is the fundamental period of the analysis model computed using eigenvalue analysis. While the overstrength 'Ω' is the ratio between the maximum base shear ($V_{max}$ ), to the effective design base shear ($V_d$) as shown in Equation 3:

$$\Omega = Vmax / Vd \quad (3)$$

'R' factor will be the product of the '$R_\mu$' and overstrength 'Ω', and 'P' factor shall be equivalent to 'R' for different performance levels, the relation between $R_\mu$ and μ is well established (Newmark & Hall, 1982):

$$R = R\mu * \Omega \quad (4)$$

## 4. STRUCTURAL SYSTEMS AND MODELLING

A wide range of medium and high-rise buildings has been selected for this study with different heights (10 stories, 15 stories, 20 stories). Three-dimensional models were developed to study the chosen structures' behavior by using the structural analysis and design program ETABS (CSI, 2017). The selected structures used in this study are RC moment frames categorized into four groups. Group (A) for regular structures, group (B) for vertical geometric irregularity structures with setbacks, group (C) for soft-story structures (variable heights), group D for mass irregularity structures (mass concentration).

All of these models and structures were designed and detailed according to Egyptian code (ECP, 2007, 2012) having a typical floor height of 3m, building's layout is bi-symmetric in plan, considering subsoil class D, spectrum type (1), ground acceleration (0.25g) and limited ductility class (R=5.0). Characteristic strength for concrete and yield strength for steel rebar of 30 MPa and 400 MPa, respectively, were used in the design. Columns were considered to be fixed at base, P-delta effects were considered in the analysis and design, columns and beams were idealized as frame elements connected from center to center with assigned (P-M2-M3) hinges at ends for columns and (M3) hinges at ends for beams where inelastic behavior is expected, hinge properties was computed automatically by ETABS from material and section properties according to ASCE/SEI 41-13 criteria. Loads considered in this study were, for gravity loads design included the self-weight of the structure, a typical floor cover of 2.0kN/$m^2$, partition loads of 13.5kN/m on beams with a live load of 2.0kN/$m^2$. While for seismic design purposes, masses considered in the analysis included the self-weight, floor cover, partition loads plus 25% of the live loads.

The structure was subjected to a vertical non-linear load case considering the appropriate vertical loads, then analyzed under an increasingly non-linear static load case depending on the first mode of vibration where the displacement of the of top floor was monitored with the corresponding base shear affecting the structure until a loss of strength or structural instability is reached. Figure 3 shows the general layouts and 3D models for the main structures considered in this study. Models that were designed conforming to ECP-201 FBD philosophy to assess their performance level are the ones with the (*) notations. ETABS can provide the analysis output in the form of a pushover curve representing the base reaction versus the monitored displacement; it can also be shown in the ADRS format as a relation between the spectral acceleration and the spectral displacement. Moreover, the demand spectrum can be shown on the plot with tabulated values of the capacity spectrum (ADRS capacity and demand curves), the effective damping, and the effective period can be viewed. The sequence of hinge formation and the color-coded state of each hinge can be displayed graphically in addition to its performance level according to the selected criteria, on a step-by-step basis, for each step of the static nonlinear case.

The main goal of this study is to cover a wide range of different performance levels of structures. Throughout this study, the cross-sections and reinforcement ratios were changed between two limits, namely the lower and upper limit, to appropriately reach different performance levels. The lower limit was considered by limiting the design to the vertical load combinations only, where the minimum concrete sections and reinforcement ratios can be reached to sustain the safety of the structure under gravity loads. While the upper limit was considered by designing the structures based on the Egyptian code lateral and vertical load combinations, where the largest concrete sections and reinforcement ratios can be reached. These limits have been placed to limit variations in performance levels to be based on seismic effects only while considering the lower limit models to be the least performance level that can be reached for such structures even if it is not collapse prevention levels. Table 2 below describes the studied models' geometry. Performance objective was considered according to the global overall building drift and the local structural elements damage based on the hinge rotation for each element. $V_{design}$ considered in this study for different models was based on the Egyptian code empirical equations.

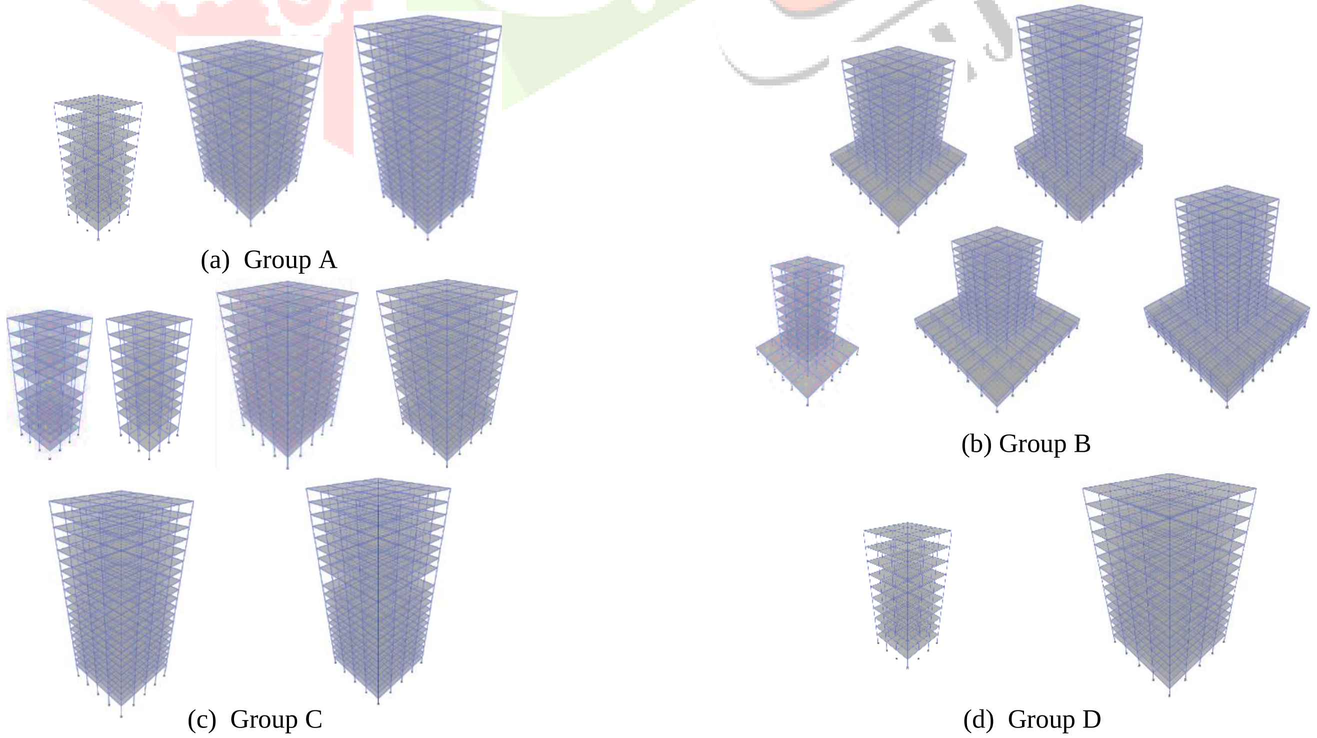

(a) Group A

(b) Group B

(c) Group C

(d) Group D

Figure 3 3D Models general layouts for the reference structures: (a) Group A, (b) Group B, (c) Group C and (d) Group D

Table 2 Structural models heights, slabs and beams concrete dimensions and structural plan dimensions

| Group | Serial | Structure Height (m) | Slab Thicknesses (mm) | Beams Dimensions (mm) | Plan Dimensions Length(m) * Width(m) |
|---|---|---|---|---|---|
| A | A.1* | 30 | 140 | 250*600 | All floors =12*12 |
| | A.2 | | | | |
| | A.3* | 45 | 160 | 250*800 | All floors =24*24 |
| | A.4 | | | | |
| | A.5 | | | | |
| | A.6* | 60 | | | |
| | A.7 | | | | |
| | A.8 | | | | |
| B | B.1* | 30 | 140 | 250*600 | 1st floor =24*24, others=12*12 |
| | B.2 | | | | |
| | B.3* | 45 | 160 | 250*800 | 1st & 2nd floors =40*40, others=24*24 |
| | B.4 | | | | 1st & 2nd floors =40*40, others=24*24 |
| | B.5 | | | | 1st & 2nd floors =40*40, others=24*24 |
| | B.6* | | | | 1st & 2nd floors =56*56, others=24*24 |
| | B.7 | | | | 1st & 2nd floors =56*56, others=24*24 |
| | B.8 | | | | 1st & 2nd floors =56*56, others=24*24 |
| | B.9* | 60 | | | 1st to 4th floors =36*36, others=24*24 |
| | B.10 | | | | 1st to 4th floors =36*36, others=24*24 |
| | B.11 | | | | 1st to 4th floors =36*36, others=24*24 |
| | B.12* | | | | 1st to 4th floors =52*52, others=24*24 |
| | B.13 | | | | 1st to 4th floors =52*52, others=24*24 |
| | B.14 | | | | 1st to 4th floors =52*52, others=24*24 |
| C | C.1* | 33 | 140 | 250*600 | All floors = 12*12, 2nd floor height=6m |
| | C.2 | | | | All floors = 12*12, 2nd floor height=6m |
| | C.3* | | | | All floors = 12*12, 5th floor height=6m |
| | C.4 | | | | All floors = 12*12, 5th floor height=6m |
| | C.5* | 48 | 160 | 250*800 | All floors = 24*24, 1st floor height=6m |
| | C.6 | | | | All floors = 24*24, 1st floor height=6m |
| | C.7 | | | | All floors = 24*24, 1st floor height=6m |
| | C.8* | | | | All floors = 24*24, 2nd floor height=6m |
| | C.9 | | | | All floors = 24*24, 2nd floor height=6m |
| | C.10 | | | | All floors = 24*24, 2nd floor height=6m |
| | C.11* | 63 | | | All floors = 24*24, 1st floor height=6m |
| | C.12 | | | | All floors = 24*24, 1st floor height=6m |
| | C.13 | | | | All floors = 24*24, 1st floor height=6m |
| | C.14* | | | | All floors = 24*24, 5th floor height=6m |
| | C.15 | | | | All floors = 24*24, 5th floor height=6m |
| | C.16 | | | | All floors = 24*24, 5th floor height=6m |
| D | D.1* | 30 | 140 | 250*600 | All floors = 12*12, 2nd floor weight doubled |
| | D.2 | | | | All floors = 12*12, 2nd floor weight doubled |
| | D.3* | | | | All floors = 12*12, 5th floor weight doubled |
| | D.4 | | | | All floors = 12*12, 5th floor weight doubled |
| | D.5* | 45 | 160 | 250*800 | All floors = 24*24, 2nd floor weight doubled |
| | D.6 | | | | All floors = 24*24, 2nd floor weight doubled |
| | D.7 | | | | All floors = 24*24, 2nd floor weight doubled |
| | D.8* | | | | All floors = 24*24, 5th floor weight doubled |
| | D.9 | | | | All floors = 24*24, 5th floor weight doubled |
| | D.10 | | | | All floors = 24*24, 5th floor weight doubled |

∗ Group: (A) regular structures, (B) structures with setbacks, (C) soft-story structures, (D) mass irregularity structures

Modern standards and guidelines allow the expression of earthquake loads (demand) by an acceleration response spectrum (ASCE, 2014; FEMA, 2005), permitting such approach the ECP horizontal response spectrum (ECP, 2012) was considered in this study as a basic representation of earthquake action for the selected buildings, as shown in Figure 4. ECP-201 divides Egypt into 6 seismic zones, as shown in Figure 5, each zone is accompanied by a different value of design ground acceleration ranging from 0.1g to 0.3g. The performance of structures was investigated using the selected demand by ASCE/SEI 41-13 target displacement procedure, which is automatically embedded in ETABS.

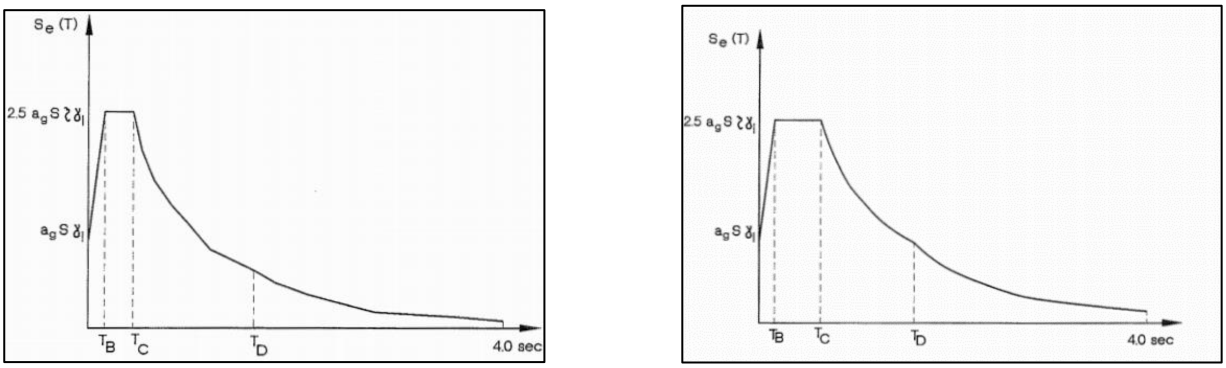


(a) Type (1) (b) Type (2)

Figure 4 Elastic horizontal response spectrum of ECP-201: (a) Type (1) and (b) Type (2)

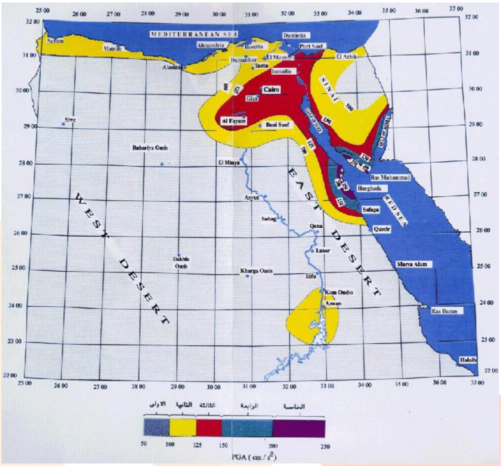


Figure 5 Seismic map of Egypt according to the current Egyptian code

## 5. STATIC PUSHOVER ANALYSIS RESULTS

The procedure used in this study distinguishes between two main points, structure properties (ductility ‘μ’ and overstrength ‘Ω’) and their performance level under the selected demand. Pushover curves obtained from nonlinear analysis were used to calculate ductility and overstrength, leading to the estimation of the ‘R’ factor, after which the performance of structure was investigated, and the ‘P’ factor for each performance level was evaluated. The results extracted from the structural models to gain insight into the structure behavior for different performance levels are shown here in this section. ECP-201 seismic provisions, which is in line with the Eurocode 8 (CEN, 2004) seismic provisions, restricts the value of the horizontal design spectrum not to be less than $0.2*a_g*\gamma_1$, where $a_g$ is the design ground acceleration and $\gamma_1$ is the structure’s importance factor, this limitation is only for structures with a fundamental period between $T_C$ and $T_D$ or structures with period exceeding $T_D$. In this study to be able to allow for more damage and reduction for the seismic forces this limit was not considered for models with life safety and collapse prevention performance levels, as this limit yields in a high design base shear values for different structures not allowing for different performance levels to be attained. Performance points of different structures were extracted from ETABS using ASCE 41-13, an example of ETABS results is shown in Figure 6 for model A.3*.

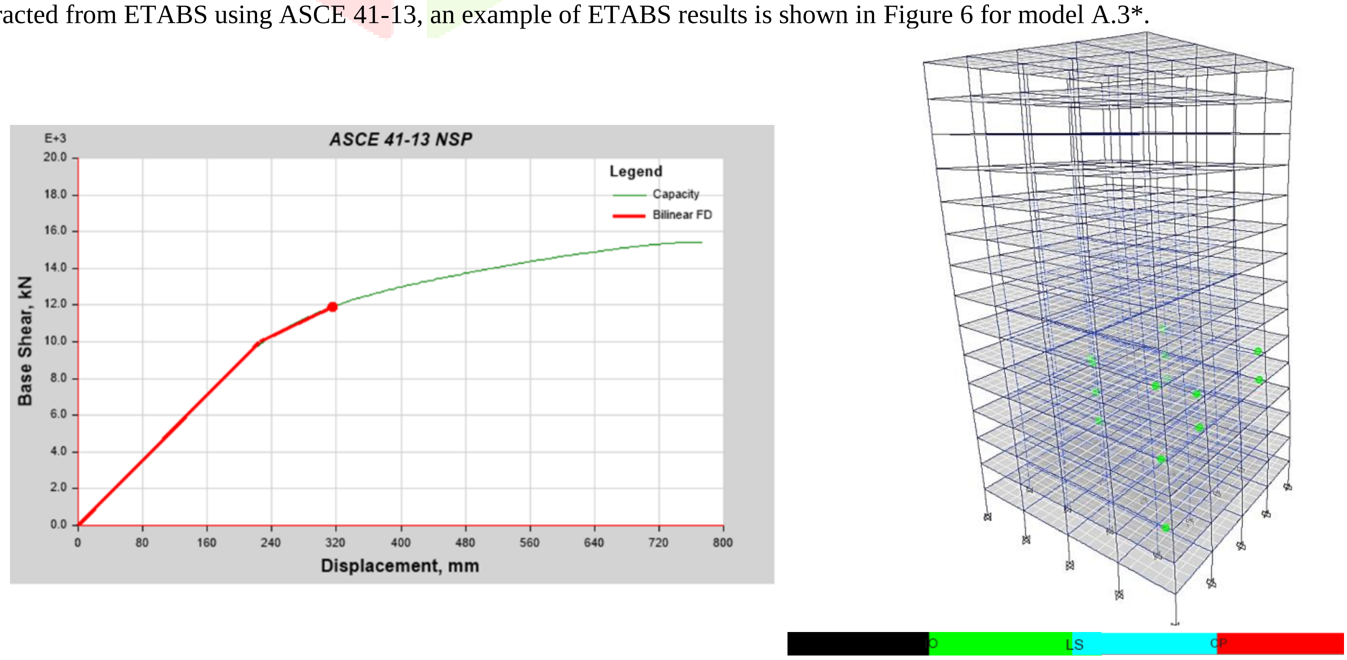


(a) ASCE 41-13 results (b) Hinge results for different elements at performance point

Figure 6 Performance point results for model A.3*: (a) ASCE 41-13 results and (b) Hinge results for different elements at performance point

### 5.1. Group A results

Group A represents the regular models considered in this study for different stories and performance levels, the results demonstrate the structure fundamental period (T), beams first hinge, columns first hinge and the performance point as shown in Figure 7 and Table 3.

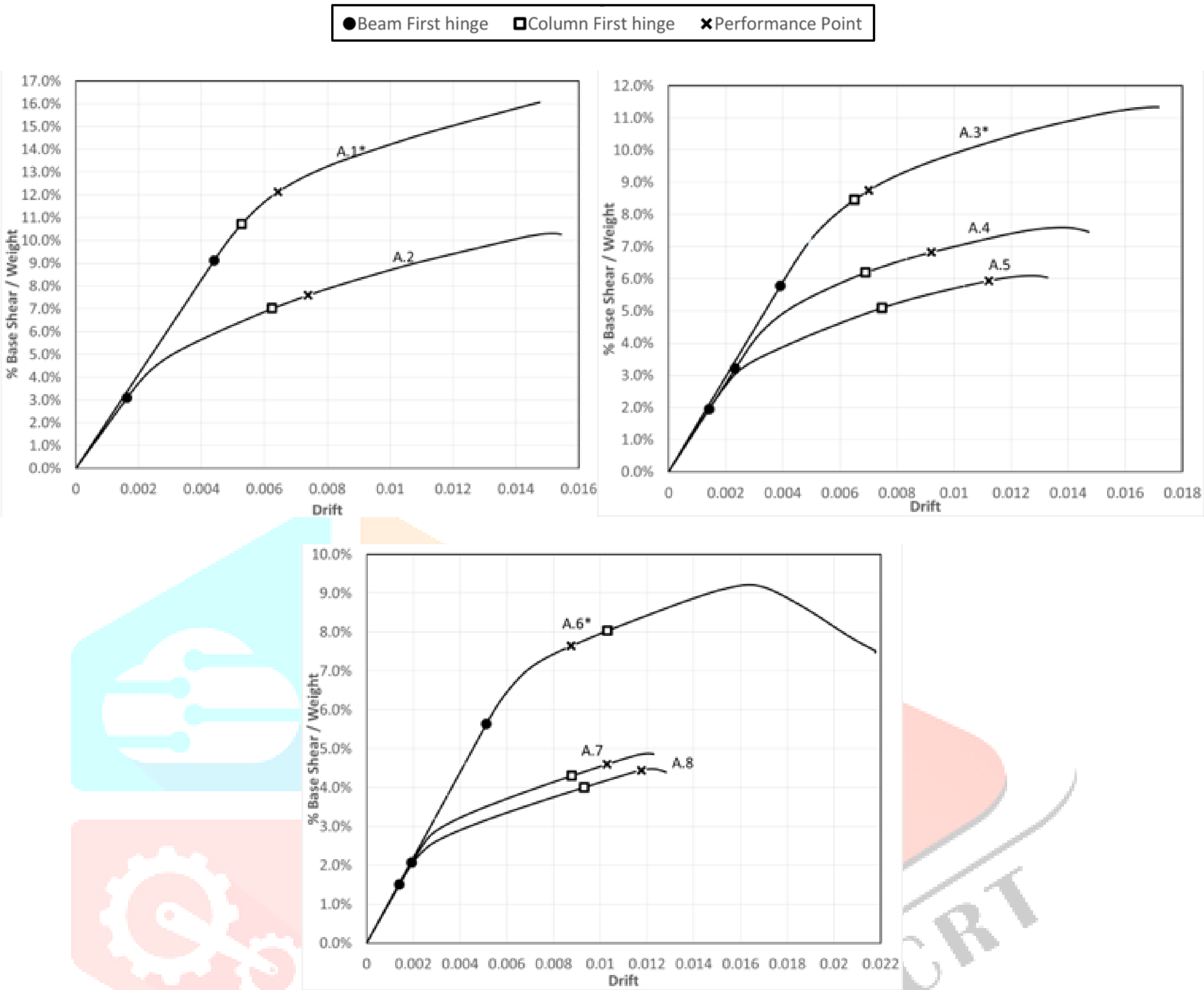


Figure 7 Group A pushover curve results and performance point

Table 3 Group A results

| Group | Serial | T (sec.) | $V_{design}$ (kN) | $V_{max.}$ (kN) | $\delta_u$ (mm) | $\delta_{y,eff}$ (mm) | $R_\mu=\mu$ | Ω | P | Performance level |
|---|---|---|---|---|---|---|---|---|---|---|
| A | A.1* | 1.85 | 1636 | 4432 | 442.7 | 178.2 | 2.48 | 2.71 | 6.73 | IO |
| | A.2 | 1.93 | 852 | 2844 | 463.1 | 163.7 | 2.82 | 3.34 | 9.45 | LS |
| | A.3* | 2.65 | 5818 | 15435 | 765.2 | 274.0 | 2.65 | 2.65 | 7.41 | IO |
| | A.4 | 2.76 | 3432 | 10342 | 662.4 | 209.8 | 3.16 | 3.01 | 9.51 | LS |
| | A.5 | 2.76 | 2646 | 8295 | 597.4 | 168.3 | 3.55 | 3.13 | 11.1 | CP |
| | A.6* | 3.56 | 7650 | 16936 | 1305 | 376.4 | 3.47 | 2.21 | 7.68 | IO |
| | A.7 | 3.62 | 3020 | 9000 | 720.0 | 223.0 | 3.23 | 2.98 | 9.62 | LS |
| | A.8 | 3.62 | 2755 | 8220 | 790.0 | 203.7 | 3.88 | 2.98 | 11.6 | CP |

Results for Group A shows the following:

- CCD models analyzed herein Group A with the (*) notation indicates that the P-Factor is varying between (6.73 and 7.7) with a performance level of IO.
- Different performance levels have been reached for different heights except for the 10 story structures as the lower limit models have yielded in a LS level due to the drift limits. Also, as the number of stories increases, the P-Factor increases.
- P-Factor for LS levels range between (9.45 and 9.62), while for CP ranges between (11.1 and 11.6).
- The maximum ratio between the base shear and structural weight decreases as the number of stories increases, for example, CCD models reached a value of 16% for 10 stories, 11.3% for 15 stories and 9.2% for 20 stories.

### 5.2. Group B results

Group B represents the irregular models with setbacks considered in this study for different stories and performance levels; the results demonstrate the structure fundamental period (T), beams first hinge, columns first hinge and the performance point as shown in Figure 8 and Table 4. Structures with setbacks chosen for this study have different geometrical configurations regarding the percentage of the setback reduction and the height at which the setback was done, as these two factors affect the behavior of such structures.

Table 4 Group B results

| Group | Serial | T (sec.) | $V_{design}$ (kN) | $V_{max.}$ (kN) | $\delta_u$ (mm) | $\delta_{y,eff}$ (mm) | $R_\mu=\mu$ | Ω | P | Performance level |
|---|---|---|---|---|---|---|---|---|---|---|
| B | B.1* | 1.85 | 1981 | 4263 | 394.5 | 146.2 | 2.70 | 2.15 | 5.81 | IO |
| | B.2 | 1.90 | 1275 | 3352 | 432.6 | 126.0 | 3.43 | 2.63 | 9.03 | LS |
| | B.3* | 2.60 | 6900 | 16610 | 733.8 | 248.2 | 2.96 | 2.41 | 7.12 | IO |
| | B.4 | 2.69 | 4085 | 11069 | 592.8 | 178.7 | 3.32 | 2.71 | 8.99 | LS |
| | B.5 | 2.69 | 2815 | 9181 | 560.0 | 153.3 | 3.65 | 3.26 | 11.9 | CP |
| | B.6* | 2.57 | 8466 | 15160 | 505.0 | 169.1 | 2.99 | 1.79 | 5.35 | IO |
| | B.7 | 2.64 | 5028 | 11356 | 589.3 | 148.7 | 3.96 | 2.26 | 8.95 | LS |
| | B.8 | 2.64 | 3133 | 9831 | 540.0 | 145.9 | 3.70 | 3.14 | 11.6 | CP |
| | B.9* | 3.32 | 9477 | 19435 | 947.0 | 315.4 | 3.00 | 2.05 | 6.16 | IO |
| | B.10 | 3.36 | 3690 | 10543 | 800.0 | 220.0 | 3.64 | 2.86 | 10.4 | LS |
| | B.11 | 3.36 | 2997 | 9112 | 705.0 | 171.3 | 4.12 | 3.04 | 12.5 | CP |
| | B.12* | 3.21 | 12472 | 20903 | 931.6 | 264.3 | 3.52 | 1.68 | 5.91 | IO |
| | B.13 | 3.23 | 4820 | 12467 | 800.0 | 219.1 | 3.65 | 2.59 | 9.44 | LS |
| | B.14 | 3.23 | 3232 | 9658 | 700.0 | 169.7 | 4.12 | 2.99 | 12.3 | CP |

Results for Group B shows the following:

- CCD models have reached an IO level accompanied by a reduction in the P-Factor from regular models (Group A) by a maximum value of 13.71% for 10 stories, 27.81% for 15 stories, 23.09% for 20 stories and to reach a minimum value of 5.35. Two main factors are affecting the behavior of such structures, the height from which the setbacks took place relative to the total building height and the size of the setbacks relative to the typical floors. These effects can be shown in structures as B.3* where even with the existence of setbacks this type of structures is not considered as an irregular one according to ECP-201, and this explains the slight decline in P-Factor (only 4 %), while for B.6* structure that exceeds the irregularity limits the decline in the P-Factor have reached a value of 27.81%.
- For the 10 story models, the lower bound limit has only reached a LS performance level due to the drift limits.
- The maximum ratio between the base shear and structural weight decreases as the number of stories increases, for example, CCD models reached a value of 13% for 10 stories, 10.22% and 7.6% for 15 stories and 8.6% and 7% for 20 stories.
- Structures with setbacks have shown a reduction in the maximum ratio between the base shear and structural weight compared with Group (A) structures; this can be attributed to the reduction found in the P-factor.

### 5.3. Group C results

Group C represents the irregular soft-story models (variable heights), considered in this study for different stories and performance levels. A variable soft-story location was assigned on different floors to study their effects on structural performance. The results demonstrate the structure fundamental period (T), beams first hinge, columns first hinge, and the performance point, as shown in Figure 9 and Table 5.

Table 5 Group C results

| Group | Serial | T (sec.) | $V_{design}$ (kN) | $V_{max.}$ (kN) | $\delta_u$ (mm) | $\delta_{y,eff}$ (mm) | $R_\mu=\mu$ | Ω | P | Performance level |
|---|---|---|---|---|---|---|---|---|---|---|
| C | C.1* | 2.26 | 1550 | 4052 | 528.0 | 230.1 | 2.29 | 2.61 | 5.99 | IO |
| | C.2 | 2.54 | 734 | 2143 | 406.0 | 154.2 | 2.64 | 2.92 | 7.69 | LS |
| | C.3* | 2.16 | 1556 | 3721 | 534.0 | 195.0 | 2.74 | 2.39 | 6.55 | IO |
| | C.4 | 2.44 | 863 | 2379 | 484.0 | 162.8 | 2.97 | 2.76 | 8.19 | LS |
| | C.5* | 2.98 | 5731 | 12144 | 614.0 | 251.6 | 2.44 | 2.12 | 5.17 | IO |
| | C.6 | 3.10 | 3082 | 9000 | 650.0 | 224.7 | 2.89 | 2.92 | 8.45 | LS |
| | C.7 | 3.10 | 1875 | 7276 | 670.0 | 181.6 | 3.69 | 3.88 | 14.32 | CP |
| | C.8* | 3.13 | 5755 | 13324 | 790.0 | 326.8 | 2.42 | 2.32 | 5.60 | IO |
| | C.9 | 3.25 | 3082 | 7950 | 700.0 | 214.7 | 3.26 | 2.58 | 8.41 | LS |
| | C.10 | 3.25 | 1844 | 6135 | 680.0 | 165.7 | 4.10 | 3.33 | 13.65 | CP |
| | C.11* | 3.77 | 7851 | 16372 | 1136 | 449.2 | 2.53 | 2.09 | 5.27 | IO |
| | C.12 | 3.88 | 2822 | 9050 | 900.0 | 283.0 | 3.18 | 3.21 | 10.20 | LS |
| | C.13 | 3.88 | 2616 | 7721 | 766.0 | 204.0 | 3.75 | 2.95 | 11.08 | CP |
| | C.14* | 3.79 | 7843 | 15624 | 1085 | 386.4 | 2.81 | 1.99 | 5.59 | IO |
| | C.15 | 3.85 | 2822 | 8468 | 850.0 | 255.0 | 3.33 | 3.00 | 10.00 | LS |
| | C.16 | 3.85 | 2760 | 7722.9 | 871.0 | 217.0 | 4.01 | 2.80 | 11.23 | CP |

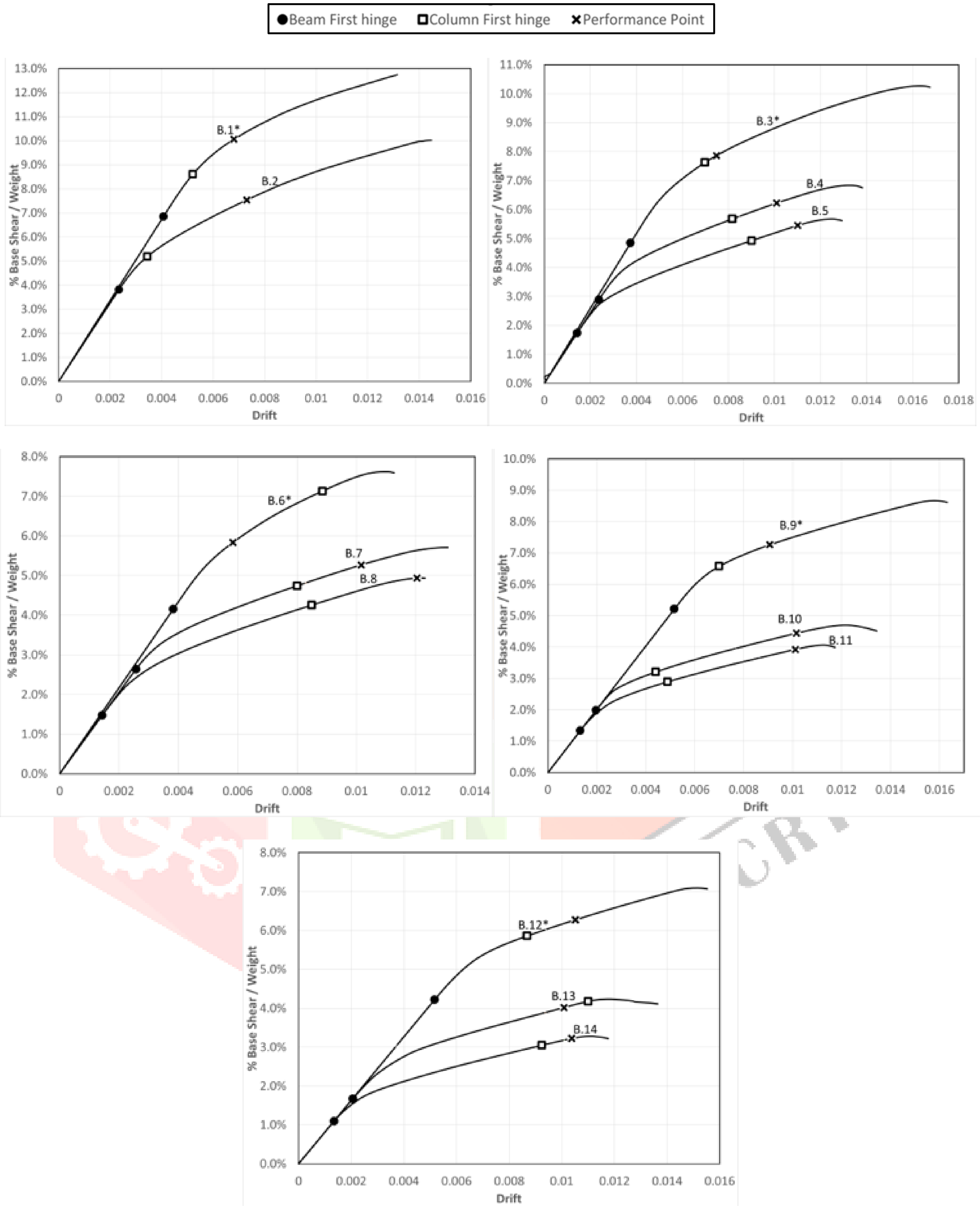


Figure 8 Group B pushover curve results and performance points

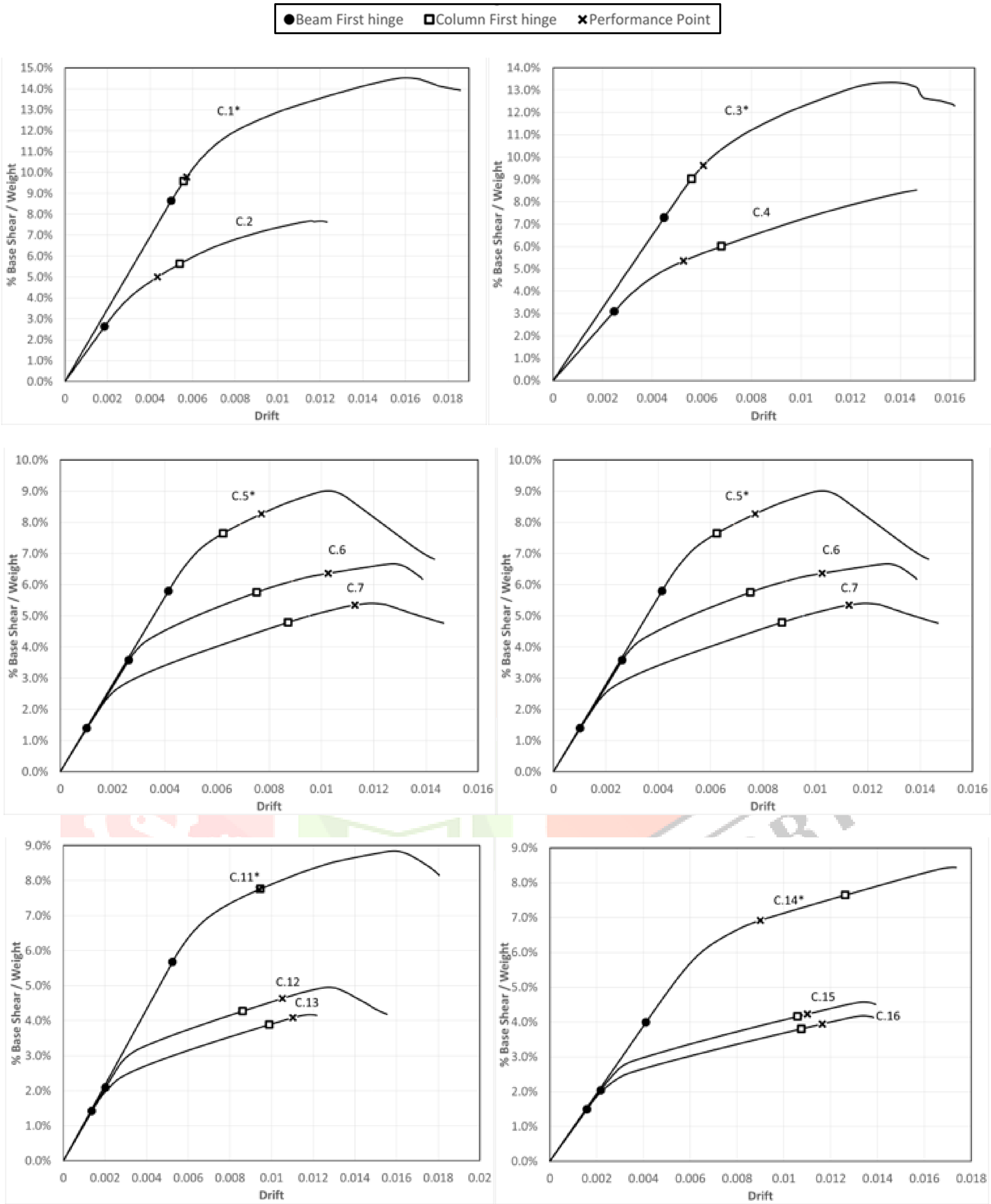


Figure 9 Group C pushover curve results and performance points

Results for Group C shows the following:

- CCD models with (*) notation have reached an IO performance level, indicating that the P-Factor has reduced from regular models (Group A) by a maximum value of 10.94% for 10 stories, 30.22% for 15 stories, 31.29% for 20 stories and to reach a minimum value of 5.17.
- The maximum ratio between the base shear and structural weight decreases as the number of stories increases, for example, CCD models reached a value of 14.5% and 13.5% for 10 stories, 9% for 15 stories and 8.25% and 8.8% for 20 stories.
- For the 10 story models, the lower bound limit has only reached a LS performance level due to the drift limits.
- P-Factor results for CCD models have shown that two factors are affecting the performance of such structures the first is the number of stories and the second is the location of the soft-story relative to the total building height, as these two factors are affecting on the percentage of reduction in the P-Factor compared with regular models. Where for structures with soft stories

located near base (C.1*, C.5*, C.11* ) the values of the P-Factor have shown a reduction by 10.94% for 10 stories, 30.22% for 15 stories and 31.29 % for 20 stories, while for structures with soft stories at mid-height (C.3*, C.8*) the reduction in the P-Factor have reached a value of 2.69% for 10 stories and 24.40 % for 15 stories, while for structures with soft stories at their top height (C.14*) the reduction in the P-Factor have reached value of 27.12%.

- P-Factor reduction values, compared to regular models, have shown that as the building height increases, the reduction values tend to increase, also when the location of the soft-story tends to be near the base the reduction values are highly increased while decreasing when theses irregularities exist in top stories.

### 5.4. Group D results

Group D represents the irregular models with mass irregularity (mass concentration), Variable mass concentration locations were assigned on different floors to study their effects on structural performance. The results demonstrate the structure fundamental period (T), beams first hinge, columns first hinge, and the performance point, as shown in Figure 10 and Table 6.

Table 6 Group D results

| Group | Serial | T (sec.) | $V_{design}$ (kN) | $V_{max.}$ (kN) | $\delta_u$ (mm) | $\delta_{y,eff}$ (mm) | $R_\mu=\mu$ | Ω | P | Performance level |
|---|---|---|---|---|---|---|---|---|---|---|
| D | D.1* | 1.86 | 1658 | 4387 | 438 | 175.9 | 2.49 | 2.65 | 6.59 | IO |
| | D.2 | 2.08 | 1110 | 2835 | 425.0 | 143.4 | 2.96 | 2.55 | 7.57 | LS |
| | D.3* | 1.87 | 1658 | 4107 | 350.0 | 166.0 | 2.11 | 2.48 | 5.23 | IO |
| | D.4 | 2.09 | 1134 | 2827 | 424.0 | 144.0 | 2.94 | 2.49 | 7.34 | LS |
| | D.5* | 2.71 | 5891 | 14591 | 707.1 | 267.8 | 2.64 | 2.48 | 6.54 | IO |
| | D.6 | 2.75 | 3587 | 10584 | 650.0 | 215.7 | 3.01 | 2.95 | 8.89 | LS |
| | D.7 | 2.75 | 3065 | 9741 | 691.0 | 198.5 | 3.48 | 3.18 | 11.06 | CP |
| | D.8* | 2.74 | 5902 | 14452 | 707.2 | 290.2 | 2.44 | 2.45 | 5.97 | IO |
| | D.9 | 2.79 | 3587 | 9913 | 590.0 | 207.0 | 2.85 | 2.76 | 7.88 | LS |
| | D.10 | 2.79 | 2700 | 8697 | 582.0 | 181.6 | 3.44 | 3.22 | 10.32 | CP |

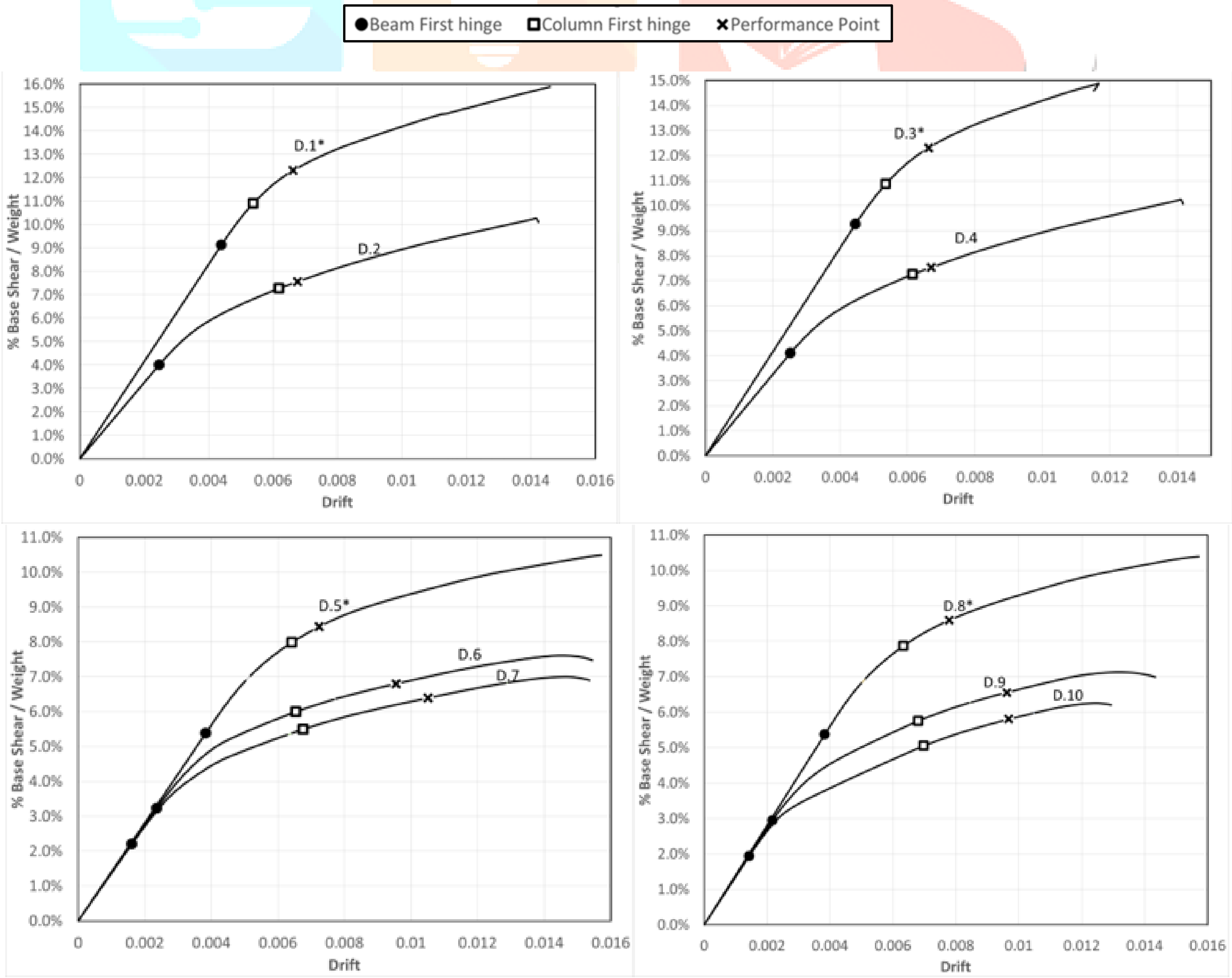


Figure 10 Group D pushover curve results and performance points

Results for Group D shows the following:

- CCD models with (*) notation have reached an IO performance level showing that the P-Factor has reduced from regular models (Group A) by a maximum value of 22.37% for 10 stories, 19.46% for 15 stories and to reach a minimum value of 5.23.
- The maximum ratio between the base shear and structural weight decreases as the number of stories increases, for example, CCD models reached a value of 16% and 15% for 10 stories, 10.5% for 15 stories.
- For the 10 story models, the lower bound limit has only reached a LS performance level due to the drift limits.
- P-Factor tends to be profoundly affected by the location of the mass concentration, as the percentage of reduction between the P-Factor for different models compared to regular models increases as the irregularity conditions are found at higher stories than at lower ones.

### 5.5. Performance evaluation

Performance results intended in this study was to provide an alternative performance-based approach for seismic design with predictable performance when subjected to earthquake effects, as code provisions provide a minimum safety level for different building ranging from tall ones to short ones without accounting for their different behavior. The main objective of this performance analysis is to control cost and predict safety margins and risk for different structures. Models performance results considered in this study were evaluated according to the overall total building drift and the hinge rotation of various structural elements, as shown in Figure 11 (ASCE, 2014), where (P) is the acceptance criteria for structural elements and (S) is for secondary elements.

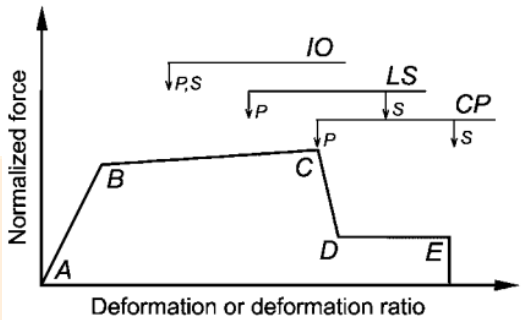


Figure 11 Generalized Component Force-Deformation Relations for Modeling and Acceptance Criteria

The results of the studied buildings in this report demonstrate the following:

- CCD models, with (*) notation, have all reached IO performance levels even for those with different irregularity conditions. Also, for regular models, the relation between the P-Factor and periodic time is shown in Figure 12 indicates that as the structural period increases, the P-Factor increases with an increase in ductility 'μ' and a decrease in overstrength 'Ω'.

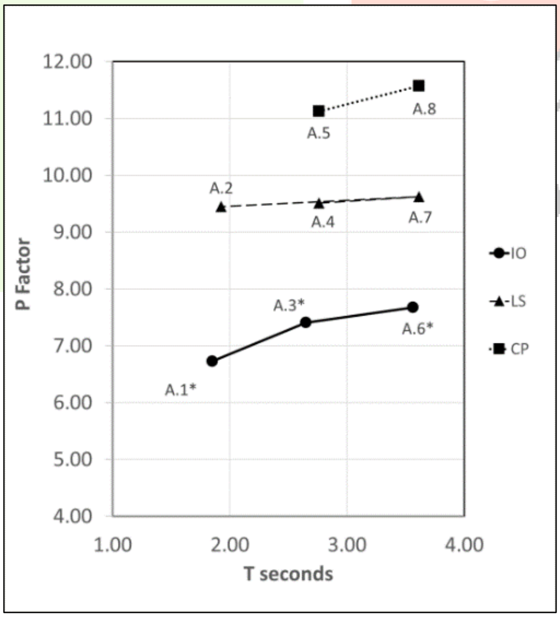


Figure 12 Relation between the P-Factor and the periodic time (T) in seconds for Group (A) structures

- ECP-201 adopts the same philosophy as Eurocode 8 regarding the setback's irregularity requirements. As for structures with setbacks the code specifies two controlling parameters to determine the vertical irregularity conditions shown in Figure 13 (a), while their effect on the studied structures is shown in Figure 13 (b), as shown in the IO results as the value of ($H_{setback}$/ $H_{building}$) increases the P-Factor value increases except at the points where the value of the setback length / total length, (L1+L3)/L as shown in Figure 13 (a), increases the P-Factor decreases conforming to the code assumptions and controlling vertical irregularity conditions.

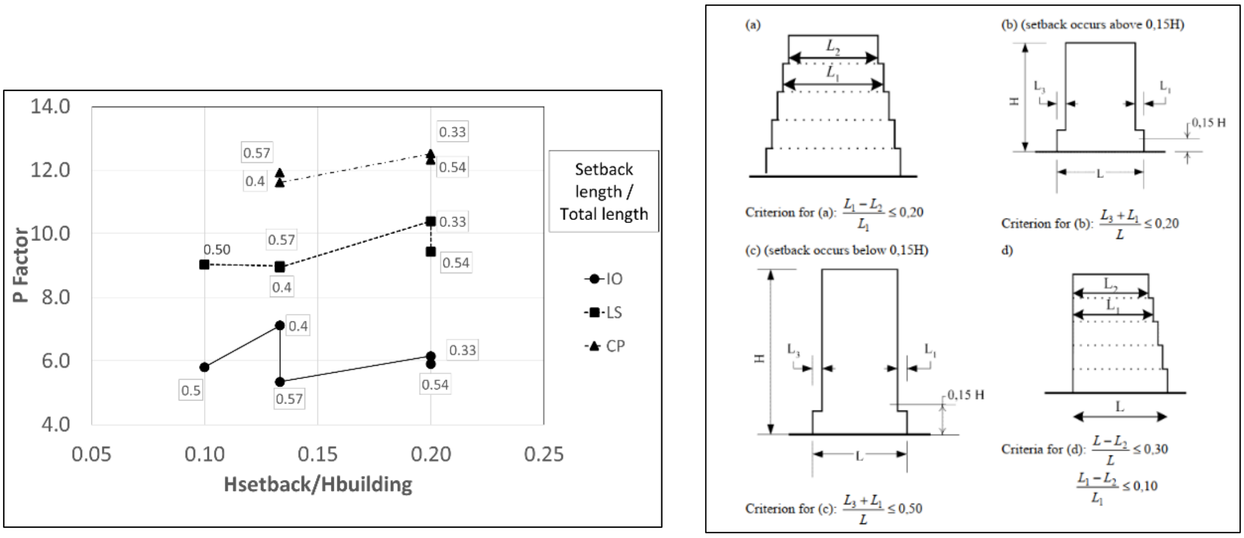


(a) Eurocode 8 Figure 4.1 (b) P-Factor value with the setback height ratio and setback dimensions ratio to the overall building dimensions

Figure 13 Group B factors affecting P-factor: (a) Eurocode 8 Figure 4.1 and (b) P-Factor value with the setback height ratio and setback dimensions ratio to the overall building dimensions

- P-Factor for Group D models is affected by the story at which the mass concentration is located, as the percentage of reduction between the P-Factor for different models, compared to regular models, increases as the irregularity conditions are found at higher stories, as shown in Figure 14.

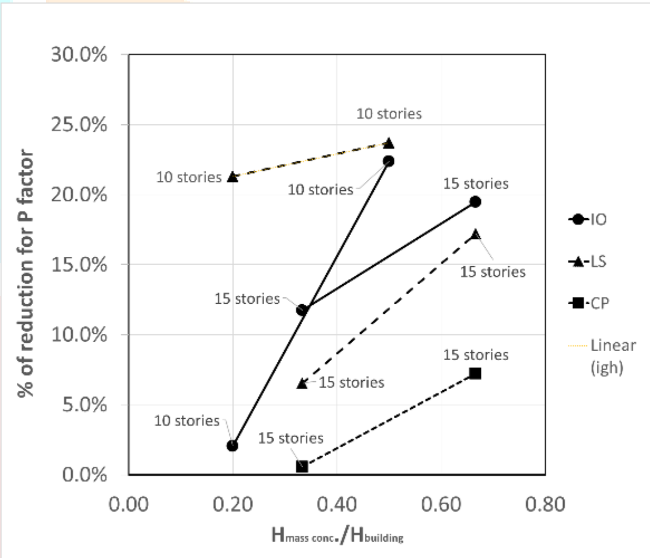


Figure 14 Group D relation between % of reduction in P-Factor and $H_{mass\ conc.}/H_{building}$

- Regular models' performance points have shown that as the number of stories increases, performance point base shear and weight ratio decreases accompanied by increasing value of building drift. Irregular models have shown reduced performance point values than regular models as for Group B the reduction depended on the degree of irregularity depending on the ratio between ($H_{setback}/H_{building}$) and the value of the setback length / total length, while for group C and D the values were affected by the location of the irregularity condition relative to the building height.

- Correlation factor (ρ) between FBD and PBD can be extracted as the value between the P-Factor at different performance levels and the code R-Factor (R=5.0) for various models as shown in Table 7.

- Beams rotations are the main factor that controls the performance levels of RC moment frames, and different reinforcement ratios can yield different performance levels.

- CP performance levels for 10 story structures cannot be reached; this is due to the lower bound limit placed in this study, which shows that the gravity load combinations found in ECP-201 (ECP, 2007) are mainly controlling the design of the 10 story structures leading to an acceptable performance level against earthquake effects.

- The range between beams and columns first yielding is broad in LS and CP models than IO models and beams first yielding occurs earlier in LS and CP models than IO models, this is due to the significant reduction of beam's reinforcement ratios found in LS and CP models than that found in IO models.

- ECP detailing requirements and seismic provisions for RC moment frames have sustained the strong column-weak beam philosophy.

Table 7 Correlation factor (ρ) for structures at different performance levels

| Groups | Correlation factor (ρ) = P / $R_{code}$ | | |
|---|---|---|---|
| | IO | LS | CP |
| A | 1.35 | 1.89 | 2.23 |
| | 1.48 | 1.90 | 2.31 |
| | 1.54 | 1.92 | |
| **Average** | **1.45** | **1.90** | **2.27** |
| B | 1.16 | 1.81 | 2.38 |
| | 1.42 | 1.80 | 2.32 |
| | 1.07 | 1.79 | 2.50 |
| | 1.23 | 2.08 | 2.46 |
| | 1.18 | 1.89 | |
| **Average** | **1.21** | **1.87** | **2.42** |
| C | 1.20 | 1.54 | 2.86 |
| | 1.31 | 1.64 | 2.73 |
| | 1.03 | 1.69 | 2.22 |
| | 1.12 | 1.68 | 2.25 |
| | 1.05 | 2.04 | |
| | 1.12 | 2.00 | |
| **Average** | **1.14** | **1.76** | **2.51** |
| D | 1.32 | 1.51 | 2.21 |
| | 1.05 | 1.47 | 2.06 |
| | 1.31 | 1.78 | |
| | 1.19 | 1.58 | |
| **Average** | **1.22** | **1.58** | **2.14** |

## 6. SUMMARY AND CONCLUSIONS

In this study, various RC moment frame structures with limited ductility class, subsoil class D, ground acceleration of 0.25g, and spectrum type (1) of the Egyptian code (ECP, 2012) were analyzed in the linear and nonlinear stages. The analysis was carried out for a wide range of buildings (10 stories, 15stories, 20stories), to correlate their results and assess their performance. Different regular (Group A) and irregular (Group B, C, D) structures were analyzed in this study, the types of irregularities considered were group B for vertical geometric irregularity models with setbacks, group C for soft-story models (variable heights), group D for mass irregularity models (mass concentration). The R-Factor considered by ECP-201 in earthquake designing was also assessed to review the Egyptian code-compliant designs (CCD), and test their effectiveness, reliability, and structural performance, and its results are shown in CCD models. The performance of the structures was carried out for all buildings according to the demand, represented here in the form of the design spectrum of ECP-201. Ductility 'μ,' overstrength 'Ω,' and 'P' factors were calculated for every intended performance level for various structures by the nonlinear static pushover analysis. Finally, the correlation factor (ρ) is introduced as the ratio between the P-Factor at different performance levels and the code R-Factor to correlate the force-based design approach with a performance-based design approach. Analysis of the obtained results has yielded in a set of conclusions, as shown below:

1. R-Factor used by ECP-201 for limited ductility RC moment frames is conservative and leads to a safe performance level, immediate occupancy level.
2. CCD models have shown good performance under earthquake effects leading to a life safe design, this was found for all regular and irregular structures considered in this study.
3. Regular models have shown higher values regarding the maximum ratio of base shear and structures weight than all other irregular models; this can be attributed to their higher P-Factor and better performance results.
4. This study has shown that structures having setbacks will yield in a more reduced performance than regular ones and that ECP-201 provisions regarding setbacks irregularity conditions are acceptable for the selected structures having different ratios of H setback/ H building and different setback length / total length.
5. Buildings with soft stories were sensitive to the location of the soft-story, where different structures have yielded in a poorer performance when the soft-story tends to be on lower floors than upper ones.
6. Buildings with mass concentration are affected by the location of the mass irregularity, where the structure has yielded in reduced performance when the mass concentration lies in higher floors rather than lower ones.
7. Irregularities considered in this study have shown that they affect the structure behavior, this can be observed in their effect on the reduction of the 'P' factor compared with regular structures, for example:
    - Group B CCD models have shown a maximum reduction ratio in the P-Factor by a value of 27.81%.
    - Group C CCD models have shown a maximum reduction ratio in the P-Factor by a value of 31.29%.
    - Group D CCD models have shown a maximum reduction ratio in the P-Factor by a value of 22.37%.
8. All different types of irregularities demonstrated in this study have shown that the code assumptions for an 'R' value of 5.0 for RC moment frame structures with limited ductility class are still valid, despite their negative impact on the structure performance.
9. Collapse prevention performance levels could not be reached for the 10 story structures showing that the Gravity load combinations found in ECP-201 (ECP, 2007) are mainly controlling the design of short-period structures yielding in concrete sections and reinforcement ratios that will achieve a life safe structural performance level.

10. Performance evaluation for different structures has been achieved and shows that as the structure height increases, the performance point base shear and weight ratio decreases accompanied by increasing value of building drift. Performance point for different irregular structures has shown a more reduced value compared with regular ones demonstrating their negative effects on the structure performance.
11. Correlation factor (ρ), (ρ) = P / R code, for different performance levels have been utilized, where for regular models it was found equal to an average value of 1.45 for IO, 1.90 for LS and 2.27 for CP levels, while for Group B it was found equal to an average value of 1.21 for IO, 1.87 for LS and 2.42 for CP levels, while for Group C it was found equal to an average value of 1.14 for IO, 1.76 for LS and 2.51 for CP levels and for Group D it was found equal to an average value of 1.22 for IO, 1.58 for LS and 2.14 for CP levels.
12. This study has indicated that P-Factor and R-Factor cannot be used as a sole resemblance factor for the structure performance, especially for models with LS and CP performance levels, as the relationship between the P-Factor of irregular models and regular ones may not always represent the negative impact of various types irregularities on the structure response. Nevertheless, upon studying the structural behavior in the non-linear stage through the performance point information, it becomes clear that the irregularities found in these structures have caused a more unsatisfactory performance level for the structure when affected by the selected demand compared with regular ones.

It is nonetheless important to realize that this study, its results, and its conclusions are so far only valid for 10, 15, and 20 story RC moment-resisting frame structures with subsoil class D, spectrum type (1) of the Egyptian code, ground acceleration (0.25g) and limited ductility class (R=5.0). Extension of these results to other seismic zones or different geometric features should be further examined in future studies.

## REFERENCES


ASCE. (2007). Seismic rehabilitation of existing buildings. *ASCE Standard*. https://doi.org/10.1201/9781439804810-c7

ASCE. (2014). Seismic Evaluation and Retrofit of Existing Buildings. *Seismic Evaluation and Retrofit of Existing Buildings*. https://doi.org/10.1061/9780784414859

ASCE. (2017a). Minimum design loads and associated criteria for buildings and other structures. *Minimum Design Loads and Associated Criteria for Buildings and Other Structures*, pp. 1–889. https://doi.org/10.1061/9780784414248

ASCE. (2017b). Seismic Evaluation and Retrofit of Existing Buildings. *Seismic Evaluation and Retrofit of Existing Buildings*. https://doi.org/10.1061/9780784414859

ATC. (1996). *Seismic evaluation and retrofit of concrete buildings (Report SSC 96-01 of California Seismic Safety Commission)*. Redwood City, CA: Applied Technology Council.

ATC. (2009). Quantification of building seismic performance factors. *Fema P695*, p. 421. Washington: Federal Emergency Management Agency.

Augusto, C., & Bhatt, F. (2011). *Seismic Assessment of Existing Buildings Using Nonlinear Static Procedures ( NSPs ) - A New 3D Pushover Procedure*. PhD dissertation, IST, Lisbon.

Belejo, A., & Bento, R. (2015). Evaluating the efficiency of recent nonlinear static procedures on the seismic assessment of an asymmetric plan building. In G. P. Cimellaro, S. Nagarajaiah, & S. K. Kunnath (Eds.), *Geotechnical, Geological and Earthquake Engineering* (Vol. 33, pp. 307–323). https://doi.org/10.1007/978-3-319-06394-2_18

béton, fib F. internationale du. (2003). Displacement-based Seismic Design of Reinforced Concrete Buildings: State-of-the-art Report. *Fib Bulletin*, *25*, 192. Retrieved from https://books.google.com/books?id=01Q6XGkw0IgC&pgis=1

CEN. (2004). European Standard EN 1998-1. Eurocode 8: Design of structures for earthquake resistance, Part 1: General rules, seismic actions and rules for buildings", Committee for Standarization. *Design*, Vol. 3. Brussels, Belgium: European Committee for Standardization.

Chaulagain, H., Rodrigues, H., Spacone, E., Guragain, R., Mallik, R., & Varum, H. (2014). Response reduction factor of irregular RC buildings in Kathmandu valley. *Earthquake Engineering and Engineering Vibration*, *13*(3), 455–470. https://doi.org/10.1007/s11803-014-0255-8

CSI. (2017). *ETABS – Integrated Building Design Software*. Berkeley, CA, USA: CSI.

ECP. (2007). *ECP-203: Egyptian code for design and construction of reinforced concrete structures*, *ECPCS-203*. Cairo: Housing and Building National Research Center. Ministry of Housing, Utilities and Urban Planning.

ECP. (2012). *ECP-201: Egyptian code for calculating loads and forces in structural work and masonry*. Cairo: ter. Ministry of Housing, Utilities and Urban Planning.

Fajfar, P. (2018). Analysis in seismic provisions for buildings: past, present and future: The fifth Prof. Nicholas Ambraseys lecture. *Bulletin of Earthquake Engineering*, *16*(7), 2567–2608. https://doi.org/10.1007/s10518-017-0290-8

FEMA. (1997). *NEHRP guidelines for the seismic rehabilitation of buildings, FEMA 273*. Washington: Federal Emergency Management Agency.

FEMA. (2000). Prestandard and Commentary for the Seismic Rehabilitation of Buildings. *Rehabilitation Requirements*, pp. 1–518. Washington DC.: Federal Emergency Management Agency.

FEMA. (2005). Improvement of Nonlinear Static Seismic Analysis Procedures. *FEMA 440, Federal Emergency Management Agency, Washington DC*, Vol. 440, p. 392. Retrieved from http://scholar.google.com/scholar?hl=en&btnG=Search&q=intitle:Improvement+of+Nonlinear+Static+Seismic+Analysis+Procedures#2%5Cnhttp://scholar.google.com/scholar?hl=en&btnG=Search&q=intitle:440,+Improvement+of+nonlinear+static+seismic+analysis+procedures#2

International Conference of Building Officials. (1997). *Uniform Building Code 1997* (Vol. 2). Vol. 2. International Conference of Building Officials.

Jiang, H., Lu, X., & Zhu, J. (2012). Performance-based seismic analysis and design of code-exceeding tall buildings in Mainland China. *Structural Engineering and Mechanics*, *43*(4), 545–560. https://doi.org/10.12989/sem.2012.43.4.545

Krawinkler, H., & Seneviratna, G. D. P. K. (1998). Pros and cons of a pushover analysis of seismic performance evaluation. *Engineering Structures*, *20*(4–6), 452–464. https://doi.org/10.1016/S0141-0296(97)00092-8

LATBSDC. (2018). *AN ALTERNATIVE PROCEDURE FOR SEISMIC ANALYSIS AND DESIGN OF TALL BUILDINGS LOCATED IN THE LOS ANGELES REGION*. Los Angeles, CA: Los Angeles Tall Buildings Structural Design Council.

Mehanny, S. S. F., & El Howary, H. A. (2010). Assessment of RC moment frame buildings in moderate seismic zones: Evaluation of Egyptian seismic code implications and system configuration effects. *Engineering Structures*, *32*(8), 2394–2406. https://doi.org/10.1016/j.engstruct.2010.04.014

Mwafy, A. (2013). Use of overstrength and inelastic response in seismic design. *Proceedings of the Institution of Civil Engineers: Structures and Buildings*, *166*(6), 282–297. https://doi.org/10.1680/stbu.11.00022

Mwafy, A. M., & Elnashai, A. S. (2001). Static pushover versus dynamic collapse analysis of RC buildings. *Engineering Structures*, *23*(5), 407–424. https://doi.org/10.1016/S0141-0296(00)00068-7

Newmark, N., & Hall, W. (1982). *Earthquake Spectra and Design, EERI Monograph. Earhquake Engineering Institute*. Berkeley, C.A: Earthquake Engineering Research Institute.

Priestley, M. J. N. (2003). *Myths and Fallacies in Earthquake Engineering , Revisited The Ninth Mallet Milne Lecture , 2003*. Istituto Universitario di Studi Superiori di Pavia.

TBI. (2017). Guidelines for Performance-Based Seismic Design of Tall Buildings. *PEER Report 2010/05*. Berkeley, Californi: The TBI Guidelines Working Group, Pacific Earthquake Engineering Research Center, University of California.

Uang, C. M. (1991). Establishing R (or Rw) and Cd factors for building seismic provisions. *Journal of Structural Engineering (United States)*, *117*(1), 19–28. https://doi.org/10.1061/(ASCE)0733-9445(1991)117:1(19)